Characterization of Radial and SMD Ceramic Capacitors in Microwave Frequency Range for NLTL Applications*

L. P. Silva Neto[1], P. A. G. Dias, J. O. Rossi, J. J. Barroso
Associated Plasma Laboratory
National Institute for Space Research
São José dos Campos, Brasil
[1]silvaneto007@yahoo.com.br

***Abstract*—Low loss dielectric materials with high permittivity and nonlinear behavior are essential for use in capacitive nonlinear transmission lines (NLTLs) for RF generation. NLTLs have a great potential to generate solitons waves for high power microwave applications in mobile defense platforms and satellite communications. In this work the dielectric properties of four commercial ceramic capacitors (two radial and two SMD types) based on barium titanate ($BaTiO_3$) were characterized in a broadband frequency from 10 MHz to 1.2 GHz for use in NLTLs. The characterization of materials consists of measuring the relative dielectric constant (real and imaginary parts) as function of the applied frequency to calculate permittivity and the loss tangent of the material. The SMD capacitors tested in this work showed a good performance in high frequency range with self-resonance greater than 1.0 GHz with lower losses and weak nonlinearity in a large frequency range, which is very suitable for applications in telecommunications systems such as in mobile phones, but not in NLTLs. On the other hand, radial capacitors are more suitable in NLTL applications because of their strong nonlinearity; however, their performance are compromised by the self-resonant frequency between their capacitance and the inherent parasitic inductance associated to the capacitor geometry and terminals, restricting their frequency range of operation for use in NLTLs up to 0.2 GHz.**

Keywords—ceramic capacitor; permittivity; nonlinearity; microwave; NLTLs

I. Introduction

Nowadays the search for faster, compact and powerful electronic systems, has led to the development of materials that present suitable electrical properties for reducing integrated circuits and electronic devices. In the group of these materials ferroelectric ceramics are found, which have been studied for applications in microwave due to their dielectric characteristics, such as high permittivity, low loss and high breakdown dielectric strength. The applications of electronic ceramics are well established in the industry of high voltage capacitors, faster random access memory (FRAM) and dynamic random access memory (DRAM) [1].

Dielectric ceramics are also being tested for building dielectric nonlinear transmission lines (NLTLs) for high power microwave generation to be applied in UWB radar, surveillance, remote sensing, battlefield communication disruption and space vehicles. With space application, NLTLs have been studied with the purpose of replacing the travelling wave tube amplifier (TWTA) and solid state power amplifier (SSPA) used in satellites for image transmission data, telemetry, and communications. The reason for that is because compact NLTLs do not need auxiliary high voltage sources and heating filament. As first attempt, Ikezi *et al.* [2] generated high power sub microwave signals of the order of 250-400 MHz using $BaTiO_3$ (BT) ferroelectric ceramic tiles. However, high dielectric loss prevented from achieving high modulation depth of the oscillations obtained. Recently, French *et al*. built an NLTL using a different piezoelectric material (PMN-lead manganese and niobium) as nonlinear medium for RF generation, but the results were disappointing because of the strong damped oscillations at the output due to the higher dielectric losses presented by the PMN ceramic [3].

The ferroelectric ceramics have a nonlinear behavior because of the variation of the relative permittivity with voltage, which is a primordial requirement for soliton generation in microwave or RF ranges. Described by a squared hyperbolic secant function, solitons are oscillations generated in lumped NLTLs because dielectric relative permittivity varies with the applied input pulse amplitude. These oscillations can be used as microwave signals. In principle NLTLs could provide sub-microwave peak power of tens of megawatts at a certain pulse repetition rate (0.1 – 1 kHz) with dielectric requirements of high voltage breakdown strength (BD- tens of kV/cm) and low loss tangent (< 1%). As shown elsewhere [4], [5] the capacitors based BT dielectrics have dielectric BD strength of the order of 100 kV/cm. Nevertheless, the loss tangent of these devices at sub-GHz frequencies is not provided by the suppliers. To assess BT applications in NLTLs, the materials were characterized in broadband frequency, from 0.01 GHz to 1.2 GHz, using a vector network analyzer (VNA) as show in the section of results. The complex dielectric constant of material is calculated by the reflection coefficient (S_{11}) measured using a vector network Analyzer (VNA). More details for S_{11} calculation is presented in the section III.

*Work supported by SOARD- USAF under contract number FA9550-13-1-0132.

II. Experimental set-up

Dielectric characterization in the microwave range was made using four commercial ceramic capacitors. Table I gives the dimensions and main electrical parameters for the capacitors tested. Capacitors C#1 and C#2 from Murata are radial type and have a cylindrical geometry as shown in Fig. 1 (a). Capacitors C#3 and C#4 are SMD type (surface mount device) and have rectangular shapes as described in Fig. 1(b). The commercial capacitors have dielectrics based on a ceramic mixture in which the main compound is the barium titanate ($BaTiO_3$). However, if the capacitor dielectric is class I (NPO type according to EIA standards) doping agents are used such as calcium titanate and magnesium titanate, among others, to control the temperature gradient coefficient and stabilize the relative permittivity with temperature. In fact, the dielectric composition varies greatly from one type of capacitor to another and from different manufacturers. The material compound formulation of the dielectric is not disclosed as it is proprietary to the manufacturers.

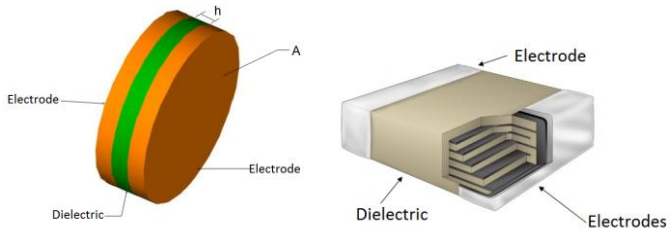

(a) (b)

Fig. 1. Shape of ceramic capacitors (a) radial (b) Surface mount device - SMD.

TABLE I. ELECTRICAL PARAMETERS AND DIMENSIONS OF CAPACITORS

Cap.	Voltage	Capacitance	Diameter	Thickness	length	width
C#1 (Y5V)	3 kV	470 pF	5.08 mm	1.18 mm	*	*
C#2 (NPO)	3 kV	100 pF	6.81 mm	0.61 mm	*	*
C#3 (NPO)	50 V	10 pF	*	2.1 mm	0.60 mm	1.25 mm
C#4 (NPO)	50 V	1 pF	*	2.0 mm	0.62 mm	1.26 mm

As general rule, dielectrics more stable with temperature are also more stable with voltage and frequency. This is the case of capacitors C#2, C#3 and C#4 that present capacitance with good stability and accuracy, being useful for higher frequency applications. Because more paraelectric material is used to stabilize the capacitance their relative permittivity is less than 600 and they are normally found up to 100 pF. As a result they have also higher resonant frequencies associated to their inherent parasitic inductance due to their planar geometry shape. Unfortunately they are not useful in NLTL applications because of their capacitance stability. On the other hand, capacitors C#1 is more suitable for these applications as it has capacitance that vary hugely with temperature, voltage and frequency. This is because more ferroelectric ceramic at ambient temperature is used in the dielectric composition. For capacitor C#1 BT is the predominant compound used in its dielectric. On the contrary to C#2, C#3 and C#4, capacitor C#1 is generally found above 300 pF with lower resonant frequencies, which limits the NLTL operation at higher frequencies (< 150 MHz). As class III capacitor C#1 (EIA standards) with type Y5V dielectric may have higher loss tangent (between 1 and 5 %) than class I stable capacitors (< 1%), which can be also other limiting factor for high frequency operation. The nonlinearity tests (CxV) of these capacitors are described elsewhere [6].

The dielectric characterization measurement in a wide range frequency from 0.01 GHz to 1.2 GHz was made using an Agilent E8364B vector network analyzer (VNA) shown in Fig. 2 (a). In this work the 50 Ω coaxial cable method for obtaining the reflection coefficient S_{11} for a PZT thin film capacitor surface in micro-strip structures (MS) and coplanar waveguides (CPW) [7], [8] is used. However, instead of using a coaxial probe on thin film surface, a micro-strip fixture as shown in Fig. 2 (b) is used to connect the component to be tested to the VNA cable. The fixture contains several micro-strip lines for the standard open-short-load calibration before carrying on with dielectric characterization measurement, as shown in Fig. 2 (b). SMA connectors located at left-side of the line tracks are used to make the connection between and the VNA 50 Ω coaxial cable and fixture. For each test, capacitor terminals were soldered onto the MS structure between copper track and ground plane at the center of the fixture for third track from bottom (see Fig. 2 (b) again). The VNA gives directly for each measurement the real (relative permittivity) and imaginary (loss) parts of S_{11}, which is used to calculate complex permittivity and dielectric loss, as shown in next section.

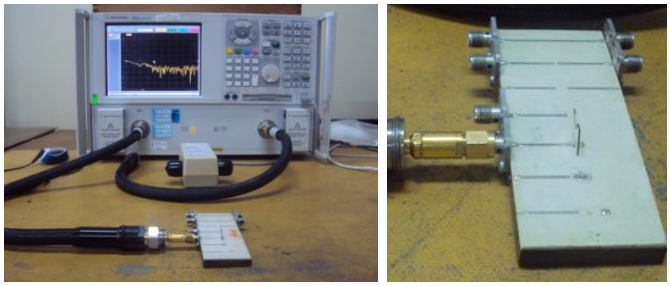

(a) (b)

Fig. 2. (a) Set-up used for dielectric characterization as a function of frequency and (b) micro-strip structure.

III. Permittivity and loss calculation

The dielectric permittivity can be expressed in the complex form as [7]

$$\varepsilon^* = \varepsilon' - j\varepsilon'' \quad (1)$$

where $\varepsilon' = \varepsilon_r$ is the real part of the relative permittivity and the imaginary part ε'' represents the dielectric losses. The dielectric losses are typically quantified in terms of the ratio between imaginary and real parts defined as loss tangent,

$$\tan\delta = \frac{\varepsilon''}{\varepsilon'} \quad (2)$$

where δ is the loss tangent angle. The capacitive impedance of the lossy dielectric is given by

$$Z = \frac{d}{(j\omega\varepsilon_0\varepsilon^* A)} \quad (3)$$

where ω is angular frequency. For the 50 Ω coaxial cable connection between fixture and VNA, the impedance of the dielectric can be calculated from the input reflection coefficient S_{11} measured as:

$$Z = 50\left(\frac{1+S_{11}}{1-S_{11}}\right) \quad (4)$$

Equating (4) to (5) obtains,

$$\frac{d}{(j\omega\varepsilon_0\varepsilon^* A)} = 50\left(\frac{1+S_{11}}{1-S_{11}}\right) \quad (5)$$

Using (5) and (6) to determine the relative permittivity and dielectric loss gives [8]:

$$\varepsilon'(\omega) = \left(\frac{d}{\omega\varepsilon_0 A}\right)\frac{1}{Z_0}\, Im\left(\frac{1-S_{11}}{1+S_{11}}\right) = k\left(\frac{-2S''_{11}}{(1+S'_{11})^2 + S''^2_{11}}\right); \quad (6)$$

$$\varepsilon''(\omega) = \left(\frac{d}{\omega\varepsilon_0 A}\right)\frac{1}{Z_0}\, Re\left(\frac{1-S_{11}}{1+S_{11}}\right) = k\left(\frac{1-S'^2_{11} - S''^2_{11}}{(1+S'_{11})^2 + S''^2_{11}}\right); \quad (7)$$

where S_{11}' and S_{11}'' are respectively the real and imaginary parts of S_{11} and $k = d/(\omega\varepsilon_0 Z_0 A)$ with $Z_0 = 50\ \Omega$.

IV. Results

With the dielectric characterization in frequency, Figs. 3 and 4 show respectively the real and imaginary parts of S_{11} measured for capacitors seen in Tab. I. However, first it is necessary to understand the S_{11} behaviour of a capacitor dielectric with losses and associated parasitic inductance. Re[S_{11}] starts from 1 with Im[S_{11}] = 0 as the capacitor is an open at low frequencies ($|S_{11}| = 1$, $\phi = 0$). As frequency is increased Re[S_{11}] and Im[S_{11}] decrease simultaneously for a smaller reactance. If frequency is still raised Re[S_{11}] and Im[S_{11}] continues to decrease with real part crossing zero and imaginary part reaching a negative peak (near -1). In the higher frequency limit the capacitor becomes a short-circuit ($|S_{11}| = 1$, $\phi = \pi$), Re[S_{11}] decreases to -1 and Im[S_{11}] tends asymptotically to zero.

Observing Figs. 3 and 4 verifies that behavior of SMD capacitors (C#3 and C#4) is according to the pattern described previously, although to C#4 capacitor the real part has not reached -1 because of the high reactance in this frequency range. Anyway, this result indicates that such capacitor has a negligible parasitic inductance in the frequency range tested and a higher resonant frequency (>>1 GHz). This is what one expects from SMD capacitor of low capacitance (1 pF) intended for microwave applications. For C#3 capacitor the imaginary part crossing zero at the frequency near to 1.0 GHz, which indicate that capacitor has electronic resonance in this frequency. For C#1 and C#2 capacitors Re[S11] goes suddenly from 1 to -1 (as in a short-circuit) with Im[S_{11}] crossing zero and becoming positive at frequencies around 0.1-0.3 GHz, which indicates that capacitors have resonant frequencies in this frequency range.

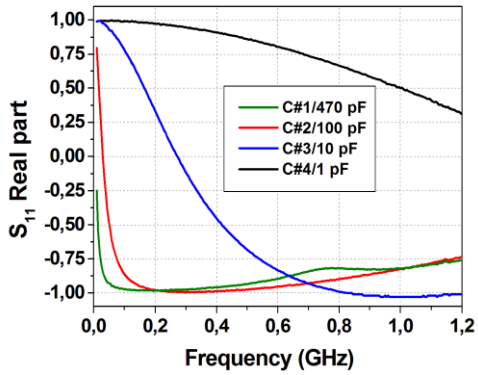

Fig. 3. Real parts of S_{11} parameter measured for all capacitors.

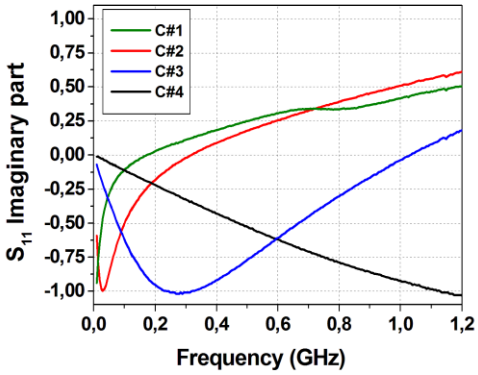

Fig. 4. Imaginary parts of S_{11} parameter measured for all capacitors.

This resonant effect can be clearly seen in Fig. 5 for capacitors C#1 and C#2 and in Fig. 6 for capacitor C#3 with real permittivity becoming negative in the curve $\varepsilon' \times f$ since above resonant frequency Im[S_{11}] is positive according to (6). For capacitor C#4 note that the relative permittivity is always positive around 500 and there is no resonance peak (no zero crossing for Im[S_{11}] in this case).

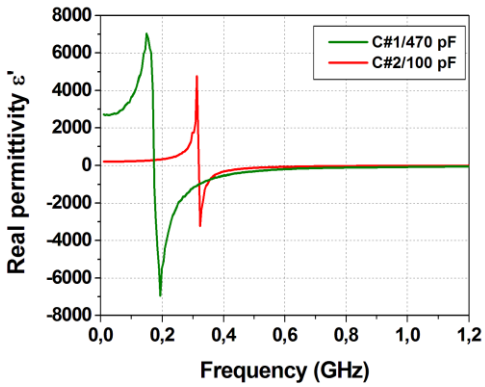

Fig. 5. Real permittivity $\times f$ calculated for radial capacitors.

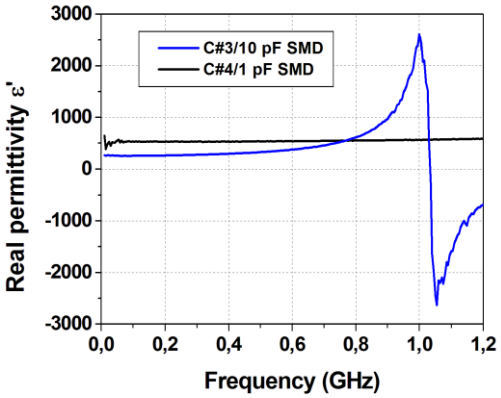

Fig. 6. Real permittivity ×*f* calculated for SMD capacitors.

The dielectric loss or tangent loss as a function of frequency can be also calculated for all capacitors using (6), (7) and (2). The results are shown in Fig. 7, where one can observe that dielectric losses are significantly lower far from the capacitor resonant frequency. At the resonant frequency there is a peak in the loss tangent curves as the capacitor becomes to a resistance since the net reactance is zero due to the associated parasitic inductance. Observe that linear capacitors (100 pF and SMD) have significant lower losses than nonlinear capacitors (470 pF), specially at lower frequencies below 0.3 GHz. For comparison, Table II gives approximately tan δ variation in the low frequency-LF and high frequency -HF) range (out the resonance) for the resonant capacitors C#1, C#2, and C#3 . For 1 pF SMD capacitor, loss tangent varied from 0.03 to 0.005 at about 300 MHz, having a good performance in relation to others, in special above 300 MHz as tan δ is kept between 0.005 and 0.06.

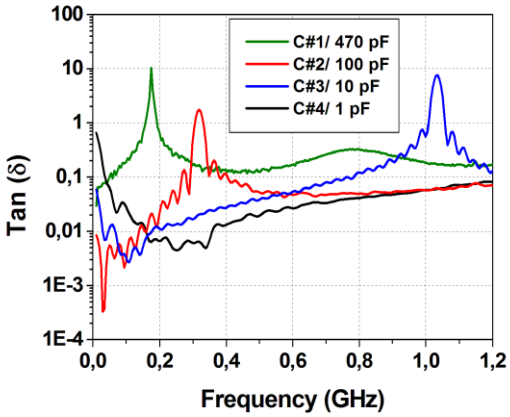

Fig. 7. Loss tangent versus *f* calculated for all capacitors.

TABLE II. LOSS TANGENT FOR RESONANT CAPACITORS

Capacitor	tan δ (LF range)	tan δ (HF range)
470 pF - Radial	0.08 – 1.0	1.0 – 0.1
100 pF - Radial	0.01 – 0.1	0.1 – 0.06
10 pF - SMD	0.003 – 0.8	0.8 – 0.2

V. Discussion of the Results

As shown in the previous section, capacitors have self-resonant frequency due to the associated parasitic inductance. As the operating frequency approaches capacitor resonance, this leads to a false increase in the permittivity (see Figs. 5 and 6). Therefore, the effective capacitance C_E near resonant frequency appears to be higher than the capacitor nominal capacitance given by [9]:

$$C_E = \frac{C_0}{1-(f/f_r)^2} \tag{8}$$

where C_0 is the nominal capacitance, f is the operation frequency, and f_r is the self-resonant frequency of the capacitor calculated as:

$$f_r = \frac{1}{2\pi\sqrt{C_0 L_s}} \tag{9}$$

The self-resonant effect can be understood by looking at the high frequency capacitor model described in Fig. 8. The real capacitor can be modeled as an ideal capacitor C_0 in series with a parasitic inductor L_s. The parasitic inductance depends on several factors: the geometric shape of capacitor, the way it was manufactured, the lead terminals and soldering connections. In the model R_p represents the lower frequency dielectric resistance due to the leakage current in the capacitor and ESR is the capacitor equivalent series resistance that includes the dielectric losses and ohmic contact resistances. R_p is normally neglected because of its value in the range of GΩ and ohmic contact resistance is in the range of hundred of milliohms for a lower loss dielectric material (tan δ< 1 %) if skin effect can be neglected. R_p and L_s do affect the effective capacitance and the quality factor Q of the capacitor is expressed as [9]:

$$Q = |X_C - X_L|/\left(R_p||ESR\right) \tag{10}$$

$$ESR = \frac{\tan\delta}{\omega C_{Vmax}} \tag{11}$$

where X_L and X_C are respectively the inductive reactance and capacitive reactance, with $C_{Vmax} = 1/2C_0$ in particular for the nonlinear capacitors C#1 and C#2 [6]. For capacitors C#3 and C#4, as it is linear $C_{Vmax} = C_0$, where C_0 is the unbiased capacitance.

As R_p>>ESR at the self resonant frequency the net reactance is zero and the capacitor becomes a pure resistance equal to ESR. Under this condition the capacitance is undefined and the capacitor is generally used in decoupling applications since ESR is in the range of mΩ. Nevertheless, above the self resonance the capacitor is in fact a DC blocking inductor and the relative permittivity becomes negative (see Figs. 5 and 6). Therefore, the NLTL must be designed at an operating frequency f_0 below f_r.

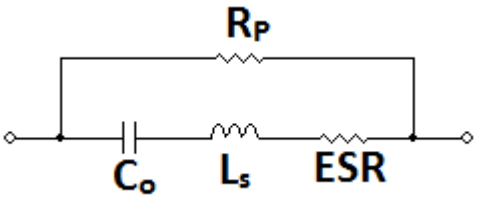

Fig. 8. Capacitor model described for operation at high frequency.

VI. Conclusions

In this work, ceramic commercial capacitors based on BT dielectrics were characterized in a frequency range between 0.01 to 1.2 GHz. The nonlinear capacitor C#1 has presented a tan $\delta > 0.1$ with ESR $\approx 1.8\ \Omega$ in the 0.075 GHz frequency range. Other important finding is that the self-resonant frequencies of radial capacitors (C#1 and C#2) limit their use in high frequency applications up to 0.1 GHz, depending on the type of capacitor used. For high frequency applications, SMD capacitors would be more appropriated, such as capacitors C#3 and C#4, which have low capacitance (10 pF and 1 pF) and consequently higher $f_r \geq 1.0$ GHz. These good results for the SMD capacitors tested (C#3 and C#4) at higher frequencies are very important for their use in microwave circuits, but not for NLTL applications as these capacitors acquired have low working voltage (50 V) and are linear (NPO type dielectric). Thus, so far to the knowledge of the authors slabs of BT inserted as capacitors in a parallel plate transmission line (as proposed by Ikezi [2]) has been the solution to minimize capacitor parasitic inductance and, consequently to obtain higher self-resonant frequencies. Other problem is that BT materials have relaxation frequency on the order of 0.8 GHz, which is other limiting factor for operation of dielectric NLTLs up to 1 GHz. One possible solution for these problems in NLTL applications could be the use of high voltage SMD capacitors of lower capacitance (< 10 pF) with self-resonant frequencies above 1GHz.

Acknowledgments

Authors thank Sergio Villela, Ivan Tosetto and Luciano Barros (DEA-INPE) for their technical assistance with the VN. Author L.P. Silva Neto also thanks Brazilian Funding Agency (CAPES) for their scholarship support.

References

[1] P.R. Arya, Pika Jha, A.K. Ganguli, "Synthesis, characterization and dielectric properties of nanometersized barium strontium titanates prepared by the polymeric citrate precursor method," Journal of Materials Chemistry, vol. 13, pp. 415-423, 2003.

[2] H. Ikezi, J.S. DeGrassie, and J. Drake, "Soliton generation at 10 MW level in the very high frequency band," Applied Physics Letters, vol.58, pp. 986-987, March 1991.

[3] D.M. French, B.W. Hoff, S. Heidger, D. Shiffler, "Dielectric nonlinear transmission line," Proceedings of the 2011 IEEE Pulsed Power Conference, pp. 341-345.

[4] J.O. Rossi .L.P. Silva Neto, and A.R. Silva Junior, "Study of HV dielectric ceramics for applications in compact pulsed power" Proceesings of the 2011 IEEE Pulsed Power Conference, pp. 459-464.

[5] L.P. Silva Neto, J.O. Rossi, and A.R. Silva Junior, "Characterization of dielectric properties of commercial ceramic capacitors for pulsed power applications," Proceedings of the 2011 IEEE Brazilian Power Electronics Conference, pp. 347-351.

[6] L.P. Silva Neto, J.O. Rossi, J.J. Barroso, A.R. Silva Jr., P.J. Castro, P.A.G. Dias, "Characterization of ceramic dielectrics for sub-GHz applications in nonlinear transmission lines" to be presented at International Microwave and Optoelectronics Conference to be held in Rio de Janeiro, August 4-7, 2013.

[7] N.F.M. Lazim, Z. Awang, Z. A. Majid, A. Yusof, and A. Dollah, " Improved characterization and modeling of PZT thin film capacitors" Proceedings of the IEEE 2007 Asia-Pacidic Conference on Applied Electromagnetics.

[8] A.N. Al-Omari and K.L. Lear, "Dielectric characteristics of spin-coated dielectric films using on-wafer parallel-plate capacitors at microwave frequencies," IEEE Trans. on dielectrics and electrical insulation, vol.12, n.6, pp.1151-1161, December 2005.

[9] B. Carter, "How (not) to decouple high-speed operational amplifiers," Application report, Texas Instruments, SLOA069, September 2001.